Received: 5 May 2020 | Revised: 26 June 2020 | Accepted: 4 July 2020

DOI: 10.1111/1442-1984.12293

PLANT SPECIES BIOLOGY WILEY

ORIGINAL ARTICLE

Genetic, morphological, and niche variation in the widely hybridizing *Rhus integrifolia-Rhus ovata* species complex

Craig F. Barrett[1] | **Joshua Lambert**[1] | **Mathilda V. Santee**[1] | **Brandon T. Sinn**[2] | **Samuel V. Skibicki**[1] | **Heather M. Stephens**[3] | **Hana Thixton**[1]

[1]Department of Biology, West Virginia University, Morgantown, West Virginia

[2]Department of Biology and Earth Science, Otterbein University, Westerville, Ohio

[3]Division of Resource Economics and Management, West Virginia University, Morgantown, West Virginia

Correspondence
Craig F. Barrett, Department of Biology, West Virginia University, 53 Campus Drive, Morgantown, WV 26506, USA.
Email: craig.barrett@mail.wvu.edu

Funding information
Eberly College of Arts and Sciences, West Virginia University; National Science Foundation EPSCoR Award, Grant/Award Number: 1920858

Abstract

Hybridization and introgression are common processes among numerous plant species that present both challenges and opportunities for studies of species delimitation, phylogenetics, taxonomy and adaptation. *Rhus integrifolia* and *R. ovata* are two ecologically important shrubs native to the southwestern USA and Mexico, and are known to hybridize frequently, but the morphological, genetic and ecological implications of hybridization in these species are poorly studied on a broad geographic scale. Analyses were conducted using leaf morphology, genetic variation of plastid and nuclear loci, and species distribution models for both species and their putative hybrid introgressants across 19 localities in California and Arizona, USA. These analyses revealed evidence for morphological and genetic distinction among localities comprising putative parental species, but a high degree of morpho-genetic intermediacy among localities with putative hybrids. Comparison of morphological and genetic population structure among localities revealed evidence for putative local adaptation or widespread phenotypic plasticity. Multiple regression models identified a weak but statistically significant negative association between leaf area and precipitation. Finally, species distribution modeling inferred northward range shifts over time, with both species predicted to occupy more coastal regions in the future, possibly increasing the frequency of hybridization among them. These findings underscore the importance of integrative assessment of multiple data sources in the study of hybridizing species and highlight the *R. integrifolia-ovata* complex as a powerful model for investigating the adaptive implications of hybridization.

KEYWORDS

Arizona, California, hybridization, introgression, species distribution modeling

1 | INTRODUCTION

Hybridization is a hallmark of many plant species complexes, often blurring species boundaries (Petit & Excoffier, 2009; Rieseberg & Soltis, 1991; Stebbins, 1969). The interplay between divergent selection among parental species in terms of maximizing reproductive success in a particular niche versus the frequency and extent of gene flow remains a key issue in evolutionary biology (Burke, Voss, & Arnold, 1998; Rieseberg, Whitton, & Gardner, 1999; Saccheri & Hanski, 2006; Slatkin, 1987; Sork, 2016). The potential outcomes of hybrid introgression are diverse

and context dependent, including: (a) lower fitness among hybrid offspring reinforcing species boundaries among distinct parental species, and leading possibly to the formation of tension hybrid zones (e.g., Abbott, 2017; Aizawa & Iwaizumi, 2020; Hoskin, Higgie, McDonald, & Moritz, 2005; Rieseberg et al., 1999); (b) higher fitness among offspring in novel or intermediate environment relative to parental species, allowing occupation of intermediate, ecotonal habitats and possible formation of bounded hybrid superiority hybrid zones, ultimately leading to ecological specialization and eventual speciation (e.g., Abbott et al., 2013; Ellstrand, 2003; Mavárez et al., 2006; Rieseberg, Van Fossen, & Desrochers, 1995; Soltis & Soltis, 2009); (c) little to no fitness consequences among offspring, with introgression simply serving as a vehicle for "neutral" genetic exchange among parental species (e.g., Gavrilets & Cruzan, 1998); and (d) the exchange of novel, adaptive genetic variation via gene flow between parental species through introgressants (Arnold, 2004; Ellstrand & Schierenbeck, 2000; Hegarty & Hiscock, 2005; Ma et al., 2019).

A "classic" example of hybrid introgression is that of *Rhus integrifolia* (Nutt.) Benth. & Hook. f. ex Rothr. and *R. ovata S. Watson*, two ecologically important shrubs native to southwestern North America (Barkley, 1937; Young, 1974). Both are major structural components of coastal scrub and chaparral ecosystems, respectively, and are important in erosion control, as native ornamental shrubs/trees, and as a source of food and shelter for wildlife. *Rhus integrifolia* occupies coastal scrub habitats in California (USA), Baja California (Mexico) and outlying islands. *Rhus ovata* occurs in coastal mountains in the chaparral regions of California and northwestern Mexico and is also disjunct to interior chaparral habitats of central Arizona (USA), separated from Californian conspecifics by the Sonoran and Mojave deserts (Montalvo, Riordan, & Beyers, 2017). Both species are gynodioecious, with hermaphroditic and male-sterile individuals frequently occurring in the same populations. This reproductive strategy has evolved numerous times in plants and is hypothesized to promote outcrossing and thereby reduce the deleterious effects of inbreeding depression (Barkley, 1937; Barrett, 2002; Freeman, Doust, El-Keblawy, Miglia, & McArthur, 1997; Munz & Keck, 1959; Young, 1972, 1974).

Rhus integrifolia has relatively small, flat, often toothed, obovate-obelliptic leaves (3–6 cm in length). *Rhus ovata* has broad, waxy, ovate-deltoid leaves that fold along the midrib of the abaxial surface into a characteristic "taco" shape, which is likely to be an adaptation to hot, arid summers in mid-lower montane chaparral zones (leaves 4–11 cm in length). These morphologies may represent extremes on an environmental continuum based on proximity to the Pacific Ocean, moisture and temperature fluctuations in a diverse, heterogeneous range from coastal California and Baja California to interior Arizona (Montalvo et al., 2017; Young, 1974). Californian populations of these two species show varying degrees of morphological intermediacy due to introgression at intermediate elevations (Figures 1; Figure S1), where they are often sympatric; that is, in regions where the mountains abruptly meet the coast (Barkley, 1937; Young, 1974). Arizonan populations of *R. ovata*, on the other hand, are allopatrically separated from *R. integrifolia* or any putatively introgressant populations of *R. ovata*, and thus may represent a "pure" form of *R. ovata*.

The two species are estimated to have diverged ca. 3 million years ago (mya) ± 1.6 mya (Miller, Young, & Wen, 2001; Yi, Miller, & Wen, 2004). Fossils attributed to both species have been found at inland sites in Nevada, farther north than the current distribution of either species, dating back to the Miocene and even Pliocene (Young, 1974). Thus, these two species may have undergone several periods of contracting and expanding distributions, being both allopatric and sympatric over hundreds of thousands to a few million years, for example, spanning several of the Pleistocene glaciations.

Young (1972, 1974) conducted meticulous studies of the breeding systems and patterns of introgressive hybridization in these two species, based on samples

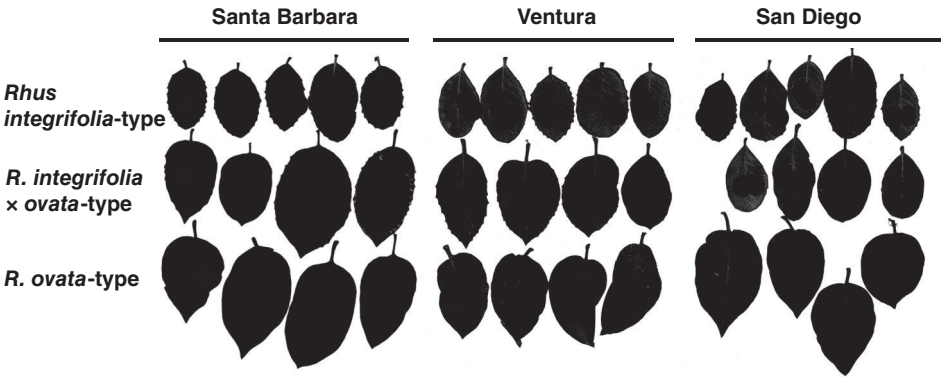

FIGURE 1 Leaf silhouette exemplars from three localities with evidence of introgression in Santa Barbara, Ventura and San Diego counties, California, USA, showing *Rhus integrifolia*-type, *R. ovata*-type and *R. integrifolia* × *ovata*-type leaf morphologies

from two "pure" localities of each species and one sympatric locality, demonstrating intermediacy in leaf and floral traits in the sympatric population. However, Young (1974) conceded that the two "pure" populations of *R. ovata* displayed some intermediate features akin to *R. integrifolia*, and could not rule out that these populations may be the result of either "ancient" introgression or introgression in the immediate past followed by backcrossing with more "pure" forms of *R. ovata*. Further, Young (1974) found limited evidence for clinal variation in leaf length and width associated with latitude within *R. ovata*, with shorter, more narrow leaves in the southernmost population compared to larger, broader leaves in the northern population, although this finding is based on comparison of only two populations.

Despite these early studies, a quantitative assessment of range-wide variation in morphology, genetic diversity and abiotic niche requirements is lacking for these two ecologically important species. Here, we use plastid and nuclear DNA sequences, leaf morphometrics, and species distribution models to characterize patterns of differentiation and hybrid introgression in the *Rhus integrifola-ovata* complex, addressing the following questions. (a) What is the extent of leaf morphological variation across the geographic ranges of *R. ovata* and *R. integrifolia*, and within introgressed populations, and how do these relate to environmental variation? (b) Do plastid and nuclear DNA show distinct patterns of population structuring across the allopatric and sympatric portions of their ranges, and what is the extent of genetic evidence for introgression? Specifically, are the disjunct Californian and Arizonan populations genetically distinct or do they display evidence of current or historical introgression (shared haplotypes) with populations in the sympatric range? (c) How do the inferred environmental niches of *R. integrifolia* and *R. ovata* differ in the present, past and future, and what is their degree of niche overlap?

2 | MATERIALS AND METHODS

2.1 | Sampling

Leaf material and voucher specimens were sampled from 19 localities across California (CA) and Arizona (AZ) (Table 1). Based on leaf morphology, localities correspond to putatively "pure" populations of *R. ovata* (n = 12), *R. integrifolia* ($n = 4$), or of "mixed" populations with signs of intermediacy (*R. integrifolia* × *ovata*; $n = 3$; Figure 1). No populations were included from the Channel Islands or Baja California due to logistical challenges of collecting.

2.2 | Morphology

Leaves were collected from the basal-most position along a branch to reduce the effect of intra-individual morphological heterogeneity. We were unable to include floral/fruit characters for every locality and instead focused on leaf characters exclusively, which have been shown to be useful indicators of introgression between *R. integrifolia* and *R. ovata* (Young, 1974). Pressed leaves were scanned at 1200 DPI on a Brother TN630 scanner along with a flat 6-cm ruler (Fisher Scientific, Waltham, Massachusetts, USA). ImageJ2 (Rueden et al., 2017) was used to measure five continuous characters: lamina length, lamina width at widest point, lamina width at 1/4 distance from apex, lamina width at 1/4 distance from base, and petiole length. We scored two meristic characters: number of secondary veins along the adaxial lamina surface on the left side, and the total number of teeth along the lamina margin. We scored seven discrete characters: teeth (present/absent); acute lamina apex (present/absent); base of lamina (acute/truncate/cordate); lamina folding (folded/flat/wavy); red lamina margin (present/absent); basal lamina lobing (present/absent); and lamina shape (ovate-deltoid/oval-elliptic/obovate-obelliptic).

We conducted principal components analysis (PCA) using a correlation matrix in PAST v.3 (Hammer, Harper, & Ryan, 2001) on all characters, and used the "biplot" function to investigate relative contributions to each resulting PC axis. We used the scree plot and "broken stick" method in PAST to assess the number of PC axes contributing significantly to the total variation. We plotted the density of individual scores along PC1 in R using the violin and jitter plot functions in the R package "ggplot2" v.3.3.1 (Wickham, 2016). We interpreted scores and density of individuals along PC1 as a proxy of a morphological hybrid index among four *a priori* groupings of taxa/localities: coastal and interior Californian *R. ovata*, coastal Californian *R. integrifolia*, interior Arizonan *R. ovata* and localities with putative introgressants (*R. integrifolia* × *ovata*). We conducted a two-way nonparametric multivariate analysis of variance (NP-MANOVA) with Gower transformation for "mixed" data (Gower, 1971) to evaluate multivariate differences in leaf morphology among groupings in PAST v.3, partitioning among two levels: grouping and locality within grouping.

2.3 | Leaf area and environmental variation

We constructed multiple regression models in order to investigate the relationship of leaf area to environmental variation. We analyzed the $\log_{10}$ leaf area, quantified using ImageJ2, and four composite environmental

TABLE 1 Collection locality information for *Rhus integrifolia*, *R. ovata* and *R. integrifolia* × *ovata*

Species present	Locality code	Locality	County, US state	*n*	Latitude, longitude	Elevation (m)
Rhus ovata	GIAZ-GL	Globe, route 77/60, Tonto National Forest	Gila, AZ	8	33.552416, −110.677328	1,330
R. ovata	GIAZ-6S	Six-shooter canyon, Tonto National Forest	Gila, AZ	6	33.339374, −110.784457	1,218
R. ovata	GIAZ-KC	Kellner canyon road, Tonto National Forest	Gila, AZ	5	33.334900, −110.830900	1,343
R. integrifolia	LACA-PV	Palos Verdes peninsula	Los Angeles, CA	7	33.743931, −118.411408	47
R. ovata	LACA-CF	Chantry flat, Angeles National Forest	Los Angeles, CA	7	34.190420, −118.022213	605
R. ovata	LACA-LH	Lake Hughes, Angeles National Forest	Los Angeles, CA	4	34.560400, −118.491109	551
R. ovata	SDCA-BG	Banner grade, route 78	San Diego, CA	6	33.084277, −116.563568	307
R. integrifolia × *ovata*	SDCA-SC	Sycamore canyon road	San Diego, CA	26	32.942893, −116.985358	289
R. ovata	SDCA-PM	Palomar Mountain, south grade, Cleveland National Forest	San Diego, CA	7	33.305918, −116.871002	1,401
R. integrifolia	SDCA-EF	Elfin Forest road	San Diego, CA	8	33.086753, −117.147970	150
R. ovata	SDCA-RG	Rainbow Glen road	San Diego, CA	10	33.415497, −117.174885	402
R. ovata	SBCA-CS	Cold Spring Trail, Los Padres National Forest	Santa Barbara, CA	8	34.458688, −119.648858	394
R. ovata	SBCA-ST	Snyder trail, Los Padres National Forest	Santa Barbara, CA	5	34.536375, −119.789871	520
R. integrifolia	SBCA-EC	El Capitan State Beach	Santa Barbara, CA	10	34.461526, −120.012142	12
R. integrifolia	VECA-BB	Beach to Backcountry Trail, Gaviota State Park	Santa Barbara, CA	20	34.482077, −120.236825	133
R. integrifolia × *ovata*	SBCA-BG	Los Padres National Forest, near Santa Barbara botanical garden	Santa Barbara, CA	24	34.467932, −119.708093	227
R. integrifolia × *ovata*	VECA-LJ	La Jolla canyon, Los Padres National Forest	Ventura, CA	23	34.092930, −119.039087	206
R. ovata	YAAZ-PR	Route 89, Prescott National Forest, near Prescott	Yavapai, AZ	5	34.423816, −112.553975	1,680
R. ovata	YAAZ-BA	Route 96, Baghdad, AZ	Yavapai, AZ	5	34.557514, −113.160571	1,064

Abbreviations: US state codes: CA, California, AZ, Arizona; n, number of individuals sampled.

predictor variables. We did not calculate specific leaf area (i.e., leaf area/leaf dry mass) because we were unable to dry the leaves simultaneously under identical conditions, which could have been a source of bias. Nineteen BIOCLIM environmental variables (11 temperature and eight precipitation) were downloaded for each sampling locality at 2.5 arc-minute resolution from https://www.worldclim.org using the R package "raster" v.3.1–5 (Hijmans, 2019), and PCA was conducted using a correlation matrix in PASTv.3. Temperature and precipitation variables were analyzed separately in order to investigate their effects individually. A broken-stick analysis was conducted as above, retaining the first two PCs for temperature and precipitation. In addition, a binary grouping variable (0 = absent, 1 = present; corresponding to groupings from Figure 2a) was included for each locality containing *R. ovata* (CA), *R. ovata* (AZ), *R. integrifolia* (CA) and *R. integrifolia* × *ovata* (CA) ($n = 4$ groups).

We included all combinations of PC1 (temperature), PC2 (temperature), PC1 (precipitation), PC2 (precipitation) and "group" in the models. The relative importance of each term (environmental PCs, group, and interaction terms) was assessed via significance in the models. The full model was specified as: $\log_{10}$ leaf area ~ $PC1_{temp}$ + $PC2_{temp}$ + $PC1_{precip}$ + $PC2_{precip}$ + group + interaction terms + error. Interaction terms included all pairwise

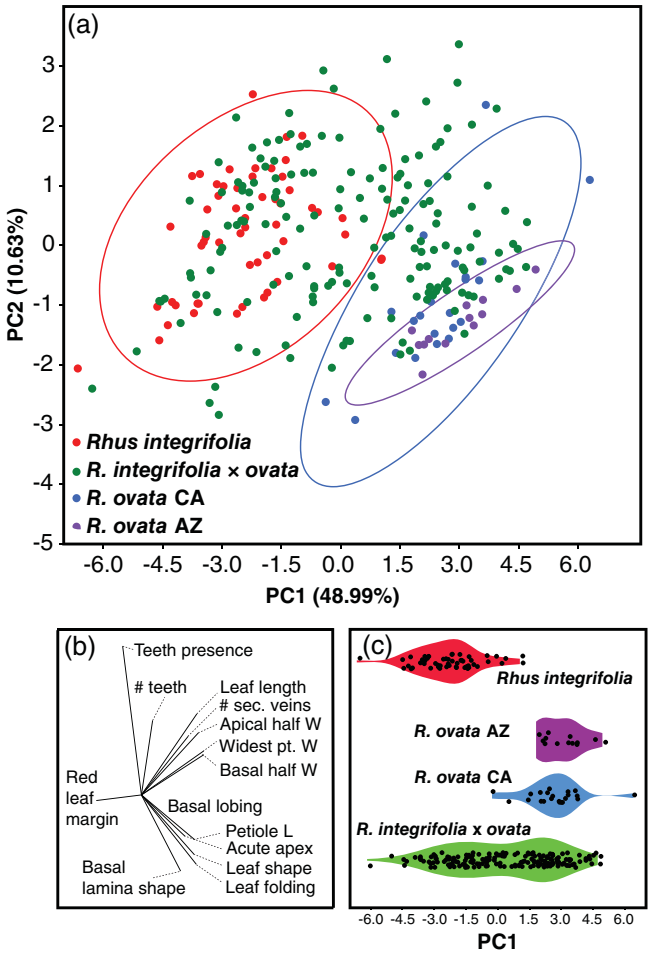

FIGURE 2 **(a)** Principal components analysis of all morphological traits based on a correlation matrix, showing the first two PCs. Percentages along axes indicate the proportion of variation explained by a particular axis. **(b)** Biplot of individual characters along PCs 1 and 2. L, length; W, width; sec, secondary. **(c)** Violin and jitter plot of individual PC scores along the first PC axis. AZ, Arizona; CA, California

combinations of temperature × precipitation PCs, and of each PC × group. Loadings scores for each BIOCLIM variable with coefficients above 0.25 were interpreted as those most strongly associated with each PC. We ran eight nested models, dropping *R. integrifolia* (CA) for those models that included a group effect. Analyses were conducted in R and tables were summarized with "jtools" v.2.0.5 (Long, 2019) and "huxtable" v.5.0.0 (Hugh-Jones, 2020), reporting R^2-adjusted values for each model, with regression coefficients, standard errors and significance for each predictor and interaction term.

2.4 | Plastid and nuclear internal transcribed spacer (ITS) variation

One cm^2 of leaf material was removed from the center of each leaf prior to pressing so as not to obscure morphological features of the leaf, and DNA was extracted following a modified hexadecyltrimethylammonium bromide protocol (Doyle & Doyle, 1987), at 1/5 volume. Total genomic DNA was subjected to PCR amplification of one nuclear and two plastid regions. We amplified the nuclear ITS with primers ITS1 and ITS4 (White, Lee, & Taylor, 1990), the plastid *ndhC-trnV*^{UAC} spacer with primers rhus-ndhC-F (5′-AGCAGAAACAT AGACGAACTCTCC-3′) and rhus-trnV-R (5′-GTCTA CGGTTCGAGTCCGTATAGC-3′), and the plastid *rpl16-rps3* intergenic spacer with primers rhus-rpl16-F (5′-GGTTCCATCGTTCCCATTGCTTCT-3′) and rhus-rps3-R (5′-TGTAGCCGCAGAATAATAAGACT-3′). These regions were chosen based on complete plastid genomes of *R. integrifolia* and *R. ovata* (NCBI GenBank accession numbers MT024991-MT024993; Barrett, unpublished data). Reactions (25 μL) included 12.5 μL Apex PCR Master Mix (Genesee Scientific, San Diego, California, USA), 9 μl H_2O, 0.2 μM of each primer, 0.5 μL 5 M Betaine, and 20-100 ng template DNA. PCR conditions for ITS consisted of 95°C for 3 min, 30 cycles of 95°C (30 s), 55°C (45 s), and 72°C (90 s), with a final extension of 72°C for 10 min. Conditions for plastid loci differed only by the annealing step (60°C for 30 s). PCR products were cleaned with 1.8x volume of AxyPrep FragmentSelect magnetic beads (Corning-Axygen, Corning, New York, USA). PCR products were cleaned with Sephadex G-50 fine medium (70 g/L; GE Healthcare, Chicago, Illinois, USA), centrifuged through a 96-well filter plate (Phenix Research, Accident, Maryland, USA), quantified via NanoDrop spectrophotometry (ThermoFisher, Waltham, Massachusetts, USA), and diluted to 30 ng/μl. PCR products were sequenced using the same primers as for amplification, following manufacturer protocols (Applied Biosystems BigDye v.3.1 cycle sequencing kit; Life Technologies, Waltham, Massachusetts, USA) on an ABI 3130XL Genetic Analyzer at the West Virginia University Genomics Core Facility.

Chromatograms were edited in Geneious R10 (http://www.geneious.com), and consensus sequences were aligned with MAFFT v.7 (Katoh and Standley, 2013) under default parameters (gap opening penalty = 2.0, offset value = 0.5). For ITS electropherograms, bi-allelic, heterozygous sites were manually scored in Geneious using IUPAC ambiguity codes. Alignments for each locus were conducted with MAFFT as above, and trimmed in Geneious to remove ambiguous calls near the priming sites. SeqPhase (Flot, 2010) and PHASE (Stephens, Smith, & Donnelly, 2001) were used to determine ITS alleles, with a 90% posterior probability per heterozygous site, using homozygous sequences as prior information. A variable minisatellite repeat in the *ndhC-trnV* spacer was coded as a single, multistate character (ATT TTT TT[K] ATT ATT AAT TAT T). Plastid loci were concatenated

and analyzed as a single alignment. Sequences are deposited in NCBI GenBank (Accession numbers: MT722227-MT722942) and alignment data deposited in Dryad (https://doi.org/10.5061/dryad.9p8cz8wdb).

Haplotype networks were constructed in PopART v.1.7 (Leigh & Bryant, 2015), using the "TCS network" option (Clement, Posada, & Crandall, 2000) with 95% connection limit. Locality codes and GPS information (decimal degrees) were then added to a NEXUS file of the plastid and ITS alignments to map haplotype frequencies using PopART and edited in Adobe Illustrator v. 24.1.1 (Adobe Inc., 2019).

2.5 | Population genetics

Population genetic analyses were conducted in ARLEQUIN v.3.5 (Excoffier & Lischer, 2010) for both plastid and nuclear datasets, estimating nucleotide diversity for each locality. Analysis of molecular variance (AMOVA; Excoffier, Smouse, & Quattro, 1992) was conducted for each dataset and partitioned by locality and grouping (as in Table 1) to quantify the proportion of variation at different hierarchical levels, and to assess the degree of population structuring across the range of this complex. Pairwise comparisons of Φ_{ST} and their significance were further conducted among localities in ARLEQUIN. The values N_{ST} and G_{ST} were compared in SPADS v.1.0 (Dellicour & Mardulyn, 2014) in order to further test significance of population genetic structure among localities. Population structure was deemed to be statistically significant if N_{ST}, which accounts for nucleotide sequence divergence, was significantly greater than G_{ST}, which treats alleles as discrete units.

We compared the relative degrees of morphological and genetic variation among localities using "Pstat" v.1.2 in R (da Silva & da Silva, 2018), which calculates "P_{ST}", an analog of "Q_{ST}", which may serve as a proxy for genetically determined morphological variation over a range of additive genetic variation and narrow-sense heritability. We used individual scores along Reist-transformed (Reist, 2011) morphological PCs 1 and 2 as metrics of morphological variation, and global estimates of Φ_{ST} from plastid and nuclear ITS, respectively. Without information from common garden and reciprocal transplant experiments, $P_{ST} > \Phi_{ST}$ may indicate localized adaptive evolution but may also reflect environmentally determined plasticity (Brommer, 2011). We used P_{ST} as an exploratory tool to distinguish a situation in which the degree of morphological variation (P_{ST}) outranks neutral genetic differentiation (Φ_{ST}) without distinguishing between genetic and environmental factors, but instead tested this relationship over a range of potential heritability.

2.6 | Species distribution modeling

Occurrence data were downloaded from the Global Biodiversity Information Facility (GBIF) using the "rgbif" v.2.3 in R. "CoordinateCleaner" v.2.0–15 (Zizka et al., 2019) was used to filter occurrence data on latitude (below 35°N, corresponding to the northern limits of the native ranges of both species), preserved specimens only, year (post-1930), missing/uncertain coordinates and range outliers.

We used the R packages "raster" (Hijmans, 2019) and 'sp' (Pebesma & Bivand, 2005) to procure 19 BIOCLIM variables from the WorldClim database (Fick & Hijmans, 2017), corresponding to the cleaned *R. integrifolia* and *R. ovata* datasets (10 km resolution), with the addition of the 19 sampled localities. We $\log_{10}$-transformed BIOCLIM data after adjusting negative and zero values (adding 100 to these). We subjected the dataset to PCA via correlation matrix in PAST, and plotted *R. integrifolia* and *R. ovata* occurrence data with the addition of new collections. We used NP-MANOVA to test for significant differences in environmental variables between *R. integrifolia* and *R. ovata* in PAST.

Species distribution models (SDMs) were inferred using MaxEnt v. 3.4.1 (Phillips, Anderson, Dudík, Schapire, & Blair, 2017; Phillips, Anderson, & Schapire, 2006) via the R package "dismo" v.1.1–4. Last Glacial Maximum (~22 kya), mid-Holocene (~6 kya), contemporary and future (IPPC5 2070) bioclimatic variable layers were obtained via WorldClim (worldclim.org) at 2.5 arcmin resolution. Last Glacial Maximum and mid-Holocene layers were generated using the Community Climate System Model v.4 (Gent et al., 2011). We assessed the impact of future climate change on species distributions by inferring future habitable ranges using both the 2.6 and 8.5 greenhouse gas representative concentration pathway (RCP) scenarios. Climate layer inclusion was filtered using Pearson correlation thresholds of 0.85 and −0.85. Analyses of niche equivalency were conducted per Barrett et al. (2019).

3 | RESULTS

3.1 | Morphology

PCA of 14 morphological characters revealed clear separation among individuals from localities hypothesized to represent "pure" forms of *R. integrifolia* and *R. ovata* in CA and AZ, as indicated by non-overlapping 95% confidence intervals (CIs) of PC axes 1 and 2 (Figure 2a). Individuals from localities with hypothesized introgression overlapped broadly in multivariate space with both

species. In other words, the *R. integrifolia* × *ovata* localities contained many individuals with PC1 scores intermediate to those of both parents, indicating they are hybrids, in addition to samples with scores falling within the range of each parental species (Figure 2c). Among localities with *R. ovata*-type morphologies, the CA and AZ individuals showed overlap, but the AZ populations occupied a small region of multivariate space, with AZ individuals contained within the 95% CI of the CA individuals. PC1 explained 48.99% of the total variation in morphological features, whereas PC2 explained 10.63% (Table 2; Table S1). PC1 was largely determined by lamina length/width characters, petiole length, the number of secondary veins, lamina apex shape, leaf folding pattern and overall leaf shape (Figures 2b; Figure S2). PC2 was largely determined by leaf shape characters (shape, folding and basal lamina) and the pattern of teeth on the lamina margin.

Morphological variation is further illustrated by a violin plot of PC1 for *R. integrifolia* vs. *R. ovata* (both CA and AZ localities), which showed clear separation among species, with individuals from introgressant populations covering the entire PC1 ranges of both (Figure 2c). Two-way NP-MANOVA suggested that groupings from Figure 2a differed significantly in multivariate leaf space (Table S2, $F = 9.897$, $p = .0001$), and that individuals from different sampling localities differed significantly within each grouping ($F = 3.511$, $p = .0001$), with no interaction among grouping and locality ($F = -11.970$, $p = 1.0$).

3.2 | Leaf area and environmental variation

Principal components analysis of 11 BIOCLIM temperature variables and eight precipitation variables indicated that the first two temperature and precipitation PCs were significant, based on a broken stick analysis (Figure S3). Based on loading scores from the PCA: $PC1_{temp}$ reflected overall temperature magnitude (60.6% of variance), $PC2_{temp}$ reflected temperature variation (31.1% of variance, e.g., isothermality, mean diurnal range and annual temperature range), $PC1_{precip}$ reflected overall precipitation magnitude (62.7% of variance) and $PC2_{temp}$ reflected variation in precipitation (24.3% of variance, e.g., precipitation seasonality; Table S3; Figure S4).

Regression models for leaf area and environmental variables are summarized in Table 3. Model 1 included the four environmental PCs and indicated a significant negative relationship between $PC1_{precip}$ and leaf area ($\beta = -0.04 \pm 0.01$, $p < .01$). Model 2 included only binary grouping variables and indicated that "group" captured a significant amount of variation in leaf area ($\beta = 0.20 \pm 0.03$; $\beta = 0.30 \pm 0.04$; $\beta = 0.33 \pm 0.05$; $p < .001$ for all). Model 3 included environmental PCs and group, further indicating that groups captured most of the variation in leaf area. Model 4 included environmental PCs and all pairwise interactions between temperature and precipitation PCs, indicating a negative association between leaf area and $PC1_{temp}$ ($\beta = -0.10 \pm 0.02$, $p < .001$); a positive

TABLE 2 Morphological character definitions and principal components analysis (PCA) loadings (PCs 1–2) based on a correlation matrix in PASTv.3

	Character type	PC 1 (48.99%)	PC 2 (10.63%)
Lamina length	Continuous	0.315	0.316
Lamina width - widest point	Continuous	0.354	0.172
Lamina width - apical halfway point	Continuous	0.325	0.243
Lamina width - basal halfway point	Continuous	0.354	0.157
Petiole length	Continuous	0.302	−0.174
Number of secondary veins (left side, adaxial surface)	Meristic	0.266	0.229
Number of teeth	Meristic	0.064	0.291
Teeth – present/absent	Binary	−0.107	0.613
Leaf apex (acute/round)	Binary	0.247	−0.161
Base of lamina (acute, truncate, cordate)	Nominal	0.223	−0.298
Folding (folded, flat, wavy)	Nominal	0.312	−0.271
Red margin (present/absent)	Binary	−0.257	−0.022
Basal lobing (present/absent)	Binary	0.054	−0.036
Lamina shape (ovate-deltoid/oval-elliptic/obovate-obelliptic)	Nominal	0.299	−0.232

TABLE 3 Multiple regression model summary for leaf area versus PCs 1 and 2 (temperature, Temp) and PCs 1 and 2 (precipitation, Precip)

	Model 1		Model 2		Model 3		Model 4		Model 5		Model 6		Model 7	
	Coef.	*SE*	Coef.	*SE*	Coef.	*SE*	Coef.	*SE*	Coef.	*SE*	Coef.	*SE*	Coef.	*SE*
(intercept)	5.91 ***	0.01	5.74 ***	0.02	5.75 ***	0.04	6.00 ***	0.04	5.84 ***	0.06	5.47 ***	0.56	5.14 ***	0.44
PC1.Temp	0.00	0.01			−0.01	0.01	−0.10 ***	0.02	−0.06	0.03	0.18	0.32	−0.01	0.02
PC2.Temp	−0.02	0.01			−0.00	0.02	0.18 ***	0.04	0.09	0.05	−0.39	0.58	−0.03	0.03
PC1.Precip	−0.04 **	0.01			−0.00	0.02	−0.06 **	0.02	−0.02	0.03	−0.08 *	0.03	0.42	0.32
PC2.Precip	0.01	0.01			−0.02	0.01	−0.05	0.03	−0.04	0.04	−0.04	0.02	−0.36	0.21
Group [2] *R. integrifolia* × *ovata*			0.20 ***	0.03	0.20 ***	0.03			0.13 **	0.04	0.65	0.58	0.78	0.43
Group [3] *R. ovata* (CA)			0.30 ***	0.04	0.32 ***	0.06			0.22 **	0.07	0.50	0.56	0.84	0.44
Group [4] *R. ovata* (AZ)			0.33 ***	0.05	0.25	0.25			0.50	0.28	−0.13	0.60	1.43 *	0.65
PC1.Temp*PC1.Precip							−0.03 ***	0.01	−0.02 *	0.01				
PC1.Temp*PC2.Precip							−0.01	0.01	−0.01	0.01				
PC2.Temp*PC1.Precip							0.02 ***	0.00	0.01 **	0.01				
PC2.Temp*PC2.Precip							−0.01	0.01	−0.00	0.01				
PC1.Temp*group [2]											−0.31	0.34		
PC1.Temp*group [3]											−0.17	0.32		
PC1.Temp*group [4]											−0.23	0.32		
PC2.Temp*group [2]											0.70	0.64		
PC2.Temp*group [3]											0.36	0.59		
PC2.Temp*group [4]											0.38	0.59		
PC1.Precip*group [2]													−0.39	0.32
PC1.Precip*group [3]													−0.52	0.32
PC1.Precip*group [4]													−0.36	0.33
PC2.Precip*group [2]													0.33	0.21
PC2.Precip*group [3]													0.30	0.21
PC2.Precip*group [4]													0.42	0.22
Model R^2 / R^2 adjusted	0.113 / 0.095		0.292 / 0.281		0.305 / 0.280		0.290 / 0.261		0.335 / 0.296		0.332 / 0.285		0.358 / 0.314	

*$p < .05$.
**$p < .01$.
***$p < .001$.
Notes: See text for further explanation of the models. Model 8 is not shown, as none of the terms were significant (including all terms and their interactions).
Abbreviations: Coef, coefficient; *SE*, standard error.

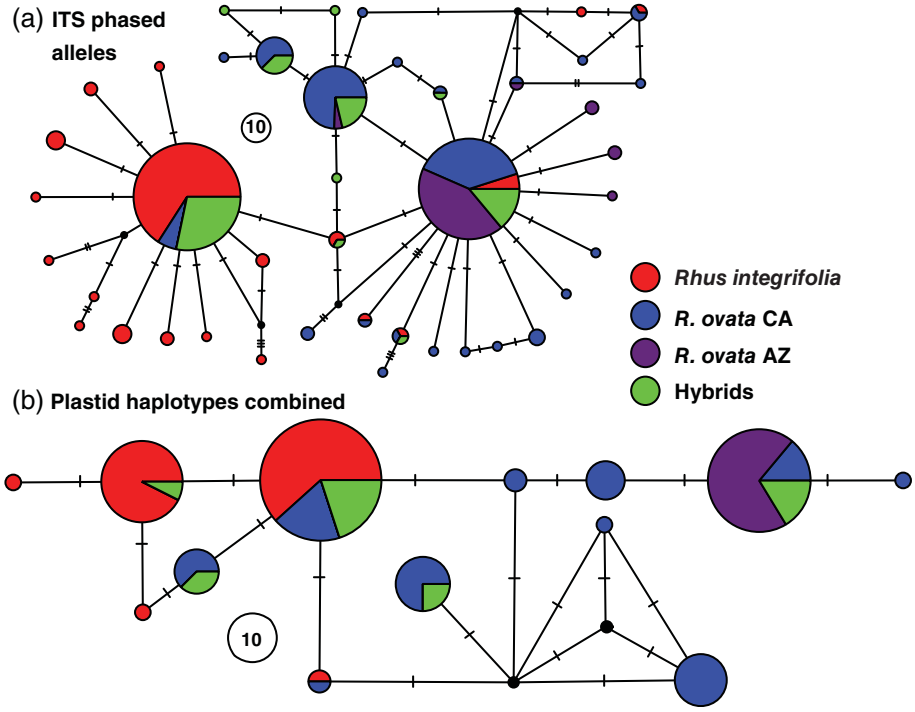

FIGURE 3 Haplotype networks for (a) nuclear ITS and (b) plastid DNA (combined *ndhC-trnV*, *rpl16-rps3*) based on TCS networks (statistical parsimony; Clement et al., 2000) with 95% connection limit. Pie charts are sampled haplotypes, colors indicate the grouping present at each particular locality, and numbered circles indicate 10 individuals (plastid DNA) or alleles (ITS). Tick marks along the network edges indicate a single nucleotide substitution between vertices. AZ, Arizona; CA, California; ITS, internal transcribed spacer

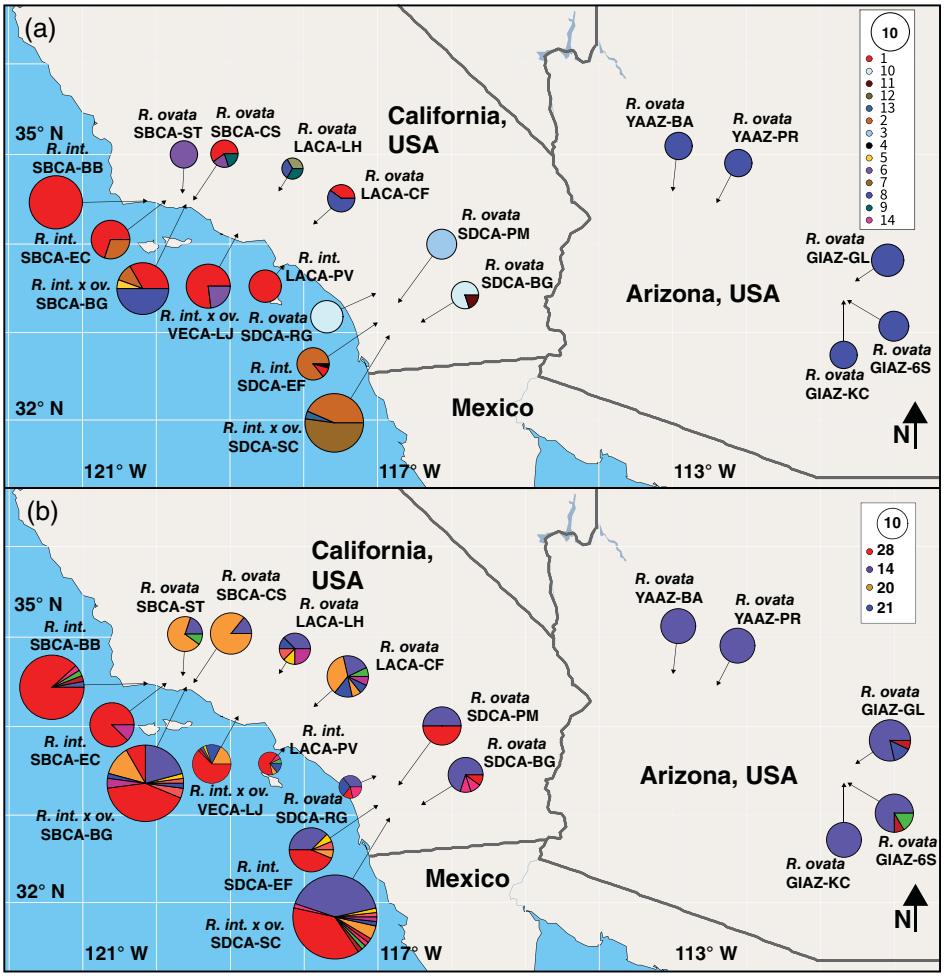

FIGURE 4 (a) Plastid and (b) nuclear ITS haplotype frequencies from 19 localities. All haplotypes are shown for plastid DNA, whereas the four most common haplotypes are shown for ITS. Localities were defined *a priori* as having only *Rhus integrifolia*, *R. ovata* or both with obvious introgressants. Locality codes correspond to county, state and locality abbreviations (e.g., GIAZ-KC = Gila County, Arizona (AZ), Kellner canyon). ITS, internal transcribed spacer

TABLE 4 Nucleotide and haplotype diversity among sampling localities

Species present	Locality code	π-Pt	A-pt	n-pt	π-ITS	A-ITS	n-ITS
Rhus integrifolia	LACA-PV	0.000	1	7	0.593	5	14
R. integrifolia	SBCA-EC	0.467	2	10	0.233	2	16
R. integrifolia	SDCA-EF	0.286	2	7	0.700	5	16
R. integrifolia	VECA-BB	0.000	1	19	0.225	4	34
R. integrifolia × *ovata*	SBCA-BG	0.660	4	18	0.771	10	48
R. integrifolia × *ovata*	VECA-LJ	0.385	2	13	0.576	6	40
R. integrifolia × *ovata*	SDCA-SC	0.561	3	23	0.691	12	58
R. ovata	SBCA-CS	0.700	3	5	0.234	2	14
R. ovata	SBCA-ST	0.650	1	5	0.511	3	10
R. ovata	SDCA-BG	0.800	2	5	0.533	4	10
R. ovata	LACA-CF	0.500	2	5	0.846	7	10
R. ovata	LACA-LH	1.000	3	3	0.857	5	8
R. ovata	YAAZ-PR	0.000	1	5	0.000	1	10
R. ovata	YAAZ-BA	0.000	1	5	0.000	1	10
R. ovata	GIAZ-GL	0.000	1	7	0.384	3	14
R. ovata	GIAZ-6S	0.000	1	6	0.439	3	12
R. ovata	GIAZ-KC	0.000	1	5	0.000	1	10
R. ovata	SDCA-PM	0.000	1	5	0.545	2	12
R. ovata	SDCA-RG	0.000	1	7	0.78	4	14

Abbreviations: π-pt, pairwise nucleotide diversity for plastid DNA; A-pt, the number of plastid haplotypes; n-pt, sample size for plastid DNA; π-ITS, pairwise nucleotide diversity for ITS; A-ITS, the number of ITS haplotypes; n-ITS, sample size for ITS; ITS, internal transcribed spacer.

association with $PC2_{temp}$ ($\beta = 0.18 \pm 0.04$, $p < .001$), and a negative relationship with $PC1_{precip}$ ($\beta = -0.06 \pm 0.02$, $p < .01$). This model also indicated a significant interaction among $PC1_{precip}$ and both temperature PCs ($\beta = -0.03 \pm 0.01$, $p < .001$ for $PC1_{temp}$; and $\beta = 0.02 \pm 0.00$, $p < .001$ for $PC2_{temp}$, respectively).

Model 5 included environmental variables, group and interactions among environmental variables. Two of the groups, *R. integrifolia* × *ovata* and Californian *R. ovata*, showed a significantly positive relationship with leaf area (coef = 0.13, standard error [*SE*] = 0.04, $p < .01$; coef = 0.22, *SE* = 0.07, $p < .01$, respectively), whereas the same two interactions showed the same significance as in Model 4. Model 6 included environmental PCs, group, and group × PC_{temp} interactions. Here, $PC1_{precip}$ had a negative association with leaf area (coef = −0.08; *SE* = 0.03, $p < .05$), whereas no other terms were significant. Model 7 was identical to model 6 but instead included group × PC_{precip} interactions; none of the terms were significant, as was the case with Model 8 (the "full" model), which included all interactions among group × environmental PCs.

3.3 | Population genetics

Figure 3 reveals 42 phased nuclear ITS haplotypes and 13 plastid haplotypes (combined *ndhC-trnV* and *rpl16-rps3*). From Figure 3, several ITS haplotypes are shared among individuals containing *R. integrifolia*, *R. ovata*, and localities with putatively introgressed individuals. A single ITS haplotype is shared by most individuals of *R. integrifolia*, with several closely related haplotypes (Figures 3 and 4). A similar pattern was observed for plastid DNA (Figures 3 and 4), with greater evidence of structuring among localities than for ITS. Five plastid DNA haplotypes are present among individuals sampled from *R. integrifolia* localities, whereas 10 are present among individuals from *R. ovata* from California. A single plastid haplotype is shared by all AZ individuals of *R. ovata*, whereas six haplotypes spanning most of the network are shared among individuals from localities containing *R. integrifolia* × *ovata*.

Overall, ITS and plastid haplotype richness is highest for *R. integrifolia* × *ovata* localities (Table 4), followed by *R. ovata* (CA), *R. integrifolia* and *R. ovata* (AZ),

TABLE 5 Analysis of molecular variance (AMOVA, in Arlequin)

Plastid	*df*	SS	*SD*	% variation	Φ	*p*
Within localities (Φ_{ST})	2	120.701	0.473	11.332	0.719	<.001
Among localities within groupings (Φ_{SC})	16	331.470	2.382	57.023	0.557	<.001
Among groupings (Φ_{CT})	152	200.881	1.322	31.644	0.364	<.001
Total	170	653.053	4.176	n/a		n/a
ITS						
Within localities (Φ_{ST})	2	284.812	1.142	36.875	0.391	<.001
Among localities within groupings (Φ_{SC})	16	90.333	0.225	7.251	0.123	<.001
Among groupings (Φ_{CT})	345	596.835	1.730	55.873	0.305	<.001
Total	363	972.000	3.0	n/a		n/a

Abbreviations: *df*, degrees of freedom; ITS, internal transcribed spacer; SS, sum of squares; *SD*, standard deviation; % variation, percent of total variation explained; 'Φ' refers to the analog of inbreeding coefficients (*F*-statistics) for haploid data; *p*, significance of differentiation at each hierarchical level.

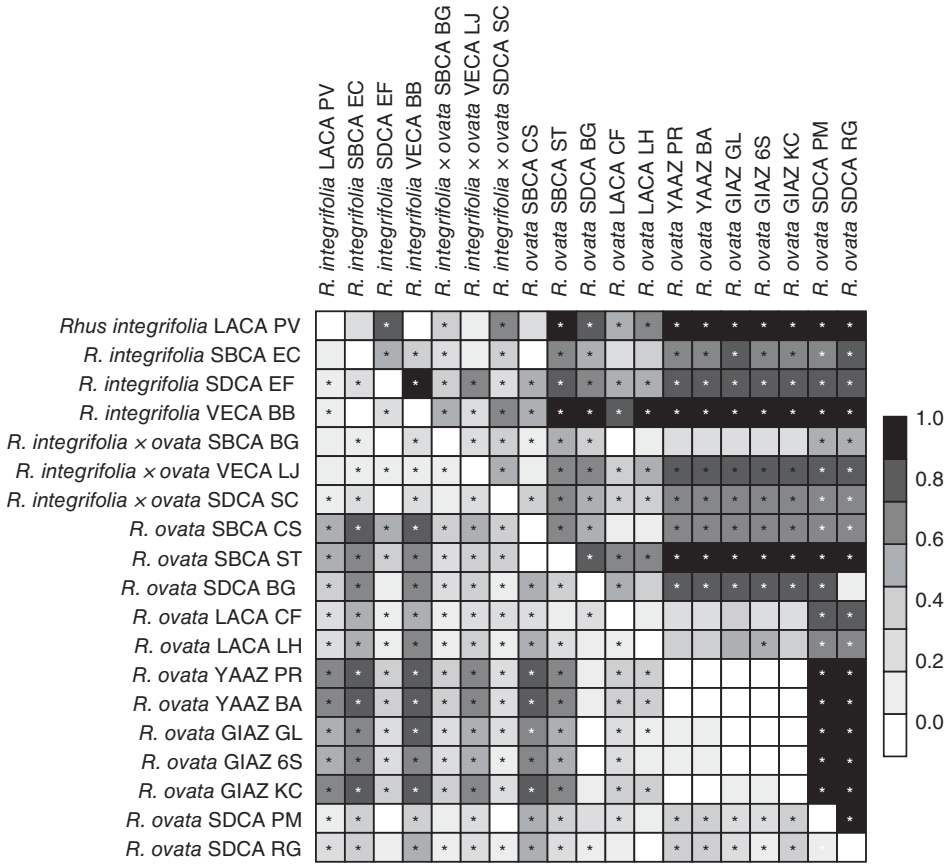

FIGURE 5 Pairwise, corrected Φ_{ST} estimates among sampling localities (conducted in Arlequin). Scale bar = Φ_{ST} value (0 to 1) and asterisks = significance at the $p < .01$ level. Above diagonal, plastid DNA; below diagonal, nuclear ITS. Rows/columns 1–4 correspond to localities with only *Rhus integrifolia*, 5–7 to those containing both species and their introgressants (*R. integrifolia* × *ovata*), and 8–19 to those containing only *R. ovata*. ITS, internal transcribed spacer

respectively. Nucleotide diversity is generally the highest in Californian *R. ovata* ($\pi_{plastid}$ range = 0.000–0.700, π_{ITS} range = 0.234–0.780) and *R. ovata* × *integrifolia* localities ($\pi_{plastid}$ range = 0.385–0.660, π_{ITS} range = 0.576–0.771), and lowest in AZ localities of *R. ovata* ($\pi_{plastid}$ = 0.000, π_{ITS} range = 0.000–0.439).

AMOVA revealed significant structure among the four groupings for ITS (Table 5; Φ_{CT} = 0.369, % variation = 55.837, $p < .001$) and plastid DNA (Φ_{CT} = 0.364, % variation = 31.644, $p < .001$). Both ITS and plastid DNA showed significant structure among localities within groupings, with plastid DNA having higher levels of structuring among localities than nuclear ITS (Table 4; for plastid DNA Φ_{SC} = 0.557, % variation = 57.023, $p < .001$; for ITS Φ_{SC} = 0.123, % variation = 7.251, $p < .001$). This pattern is further illustrated by pairwise

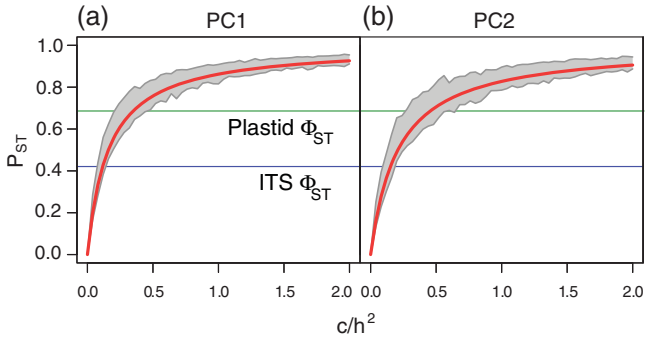

FIGURE 6 Comparisons of total morphological and neutral-genetic variation (P_{ST}-Φ_{ST}, respectively) of the first two principal component axes for morphology: (a) PC1, (b) PC2. Comparisons were grouped by sampling locality (total variation in morphology = P_{ST}), compared with global Φ_{ST} estimates for plastid DNA (green) and nuclear ITS (purple). Red line is the best fit line for P_{ST} as a function of c/h^2 (proportion of morphological variation determined by additive genetic variance/narrow-sense heritability); gray areas represent 95% confidence intervals based on 999 bootstrap replicates in the R package "Pstat" v.1.2

Φ_{ST} comparisons among localities (Figure 5). Pairwise Φ_{ST} values are generally significant and relatively high when comparing *R. integrifolia* with *R. ovata* from CA and AZ localities, but lower compared to *R. integrifolia* × *ovata* localities. A similar overall pattern is observed for ITS, but in general pairwise Φ_{ST} values are lower, reflecting the results from AMOVA of weaker overall structure among localities relative to plastid DNA. N_{ST} and G_{ST} values were 0.786 and 0.696 for plastid DNA, and 0.431 and 0.377 for ITS, respectively. For both plastid DNA and ITS, the differences between N_{ST} and G_{ST} were significant (0.090, $p < .001$; 0.054, $p < .001$, respectively).

P_{ST}-Φ_{ST} comparisons reveal differentiation in leaf morphology among localities, using the first two principal components as composite proxies (Figure 6). P_{ST} was estimated for a range of values of c/h^2, which corresponds to the ratio of additive genetic variation in morphology among localities (c) to that among individuals (h^2, i.e., narrow-sense heritability). Using the estimated global Φ_{ST} values of 0.441 for ITS and 0.684 for plastid DNA, the thresholds for c/h^2 that correspond to $P_{ST} > \Phi_{ST}$ are approximately 0.1/0.4 for PC1 and 0.2/0.5 for PC2 (for plastid DNA and ITS, respectively).

3.4 | Species distribution modeling

Filtering of occurrence data with CoordinateCleaner retained 503 of 1,209 occurrence points for *R. integrifolia* and 852 of 1,523 occurrence points for *R. ovata*. PCA of all 19 environmental variables revealed that the localities sampled only represent a subset of the total multivariate environmental niche space represented by a larger collection of herbarium records from GBIF (Figure S4). PC1 explains 46.3% of the total variation in environmental variables, and is positively associated with mean diurnal range, temperature seasonality and temperature/precipitation in the driest/warmest quarters; PC1 is negatively associated with precipitation seasonality, isothermality and temperature during the coldest month/quarter (Table S3). PC2 is positively associated with precipitation (annual, wettest month/quarter and coldest quarter) and negatively associated with temperature during the warmest/wettest quarters. Sampling localities for *R. integrifolia* × *ovata* fall at intermediate positions between those for *R. integrifolia* and *R. ovata* from California, whereas Arizonan *R. ovata* occupy a more distinct portion of multivariate space associated with warmer, more seasonal habitats (Figure S4).

Pearson analysis detected autocorrelation between many bioclimatic predictor variables. The following variables passed this autocorrelation filter and were used to infer SDMs: annual mean temperature (1), mean diurnal range (2), isothermality (3), mean temperature of warmest quarter (8), mean temperature of driest quarter (9), annual precipitation (12), precipitation of driest month (14), precipitation seasonality (15), precipitation of warmest quarter (18) and precipitation of coldest quarter (19). MaxEnt inference of species distribution models for both *R. integrifolia* and *ovata* accurately recapitulated their present ranges and showed that the historical range of *R. ovata* has been highly influenced by climate change over the past ~22,000 years (Figure 7). The average training area under curve (AUC) for the 10 replicate MaxEnt runs using contemporary climatic variables was 0.988 and 0.977 for *R. integrifolia* and *R. ovata*, respectively. Standard deviation for training AUC was less than 0.001 for each replicate.

During the Last Glacial Maximum (LGM; ca. 22 kya), areas projected to be most habitable for *R. integrifolia* were nearly restricted to Baja California (Figure 7). Contrastingly, most of the habitable range of *R. ovata* during the LGM was inferred to exist in a relatively narrow band extending from present day Arizona south to Durango, Mexico. However, the reconstructed SDM for *R. ovata* under a Mid-Holocene (ca. 6 kya) climate reflects a pronounced range shift, with most of the habitable area overlapping that of *R. integrifolia* in Baja California. *Rhus integrifolia* was inferred to gradually shift northward over time, from Baja California to the central Californian coast. *Rhus ovata* populations were inferred to have a decreasing probability of occurrence over time in Arizona, with increasing probability in coastal habitats. Perhaps most interestingly, the area including present-day Arizonan populations of *R. ovata* was inferred to be

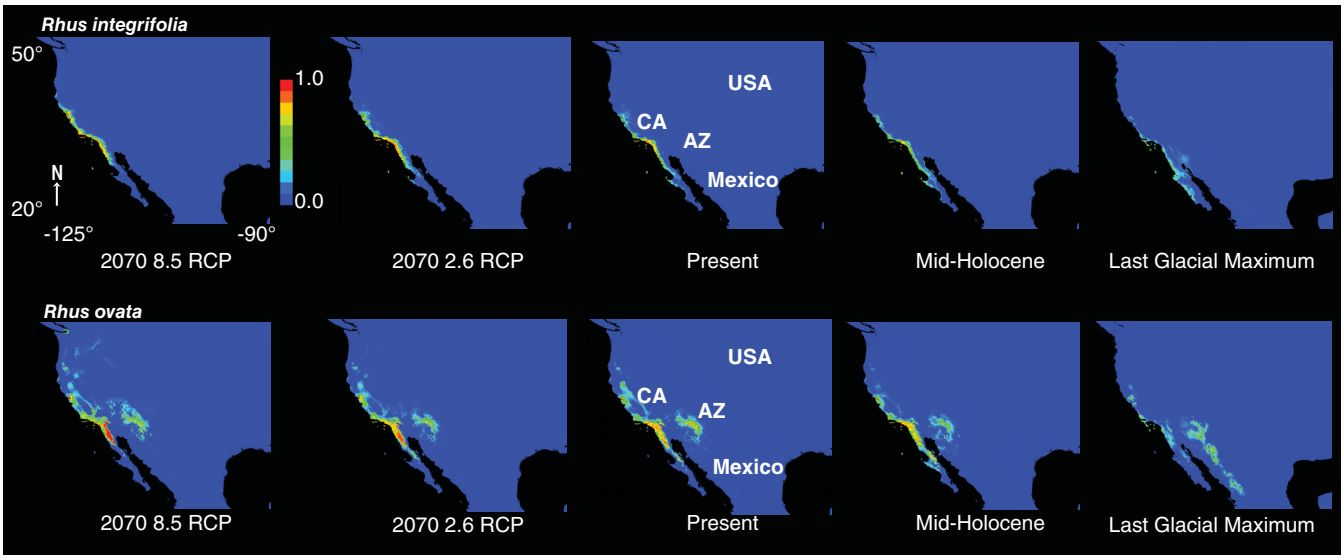

FIGURE 7 Maxent species distribution models for *Rhus integrifolia* (above) and *R. ovata* (below) at four time intervals (left to right): 2070, present-day, mid-Holocene and Last Glacial Maximum. The two models for 2070 correspond to two levels of atmospheric carbon (left 8.5 representative concentration pathway [RCP] and right 2.6 RCP). Latitude is shown on the vertical-axis, longitude on the horizontal-axis. Scale bar: probability of occurrence in each model from 0–1, where red values (top) are the highest and blue values (bottom) are the lowest

habitable since the LGM, suggesting that these populations may have become isolated from the remainder of the range sometime between 22 and 8 kya. Random translocation and rotation-multidimensional overlap (RTR-MO) analyses failed to reject niche equivalency of present ranges among *R. integrifolia* and *R. ovata* ($p = .49$). Our SDM projections suggest that the overlap in habitable range for these two species is likely to increase through 2070, regardless of the RCP scenario, as the range of *R. integrifolia* tracks northward along the California coast and the projected habitability of interior regions declines for *R. ovata*.

4 | DISCUSSION

Here, we present a geographic analysis of two ecologically important, hybridizing species, *R. integrifolia* and *R. ovata*. We present morphological and molecular evidence for distinctness among the two species, but with intermediacy in morphology and haplotype sharing for several localities where they are sympatric. We found population structure in morphology that outranks neutral genetic structure, which may indicate environmental plasticity or local adaptation. There is evidence for a negative association between overall precipitation and leaf area, but this association is amplified with increasing overall temperature and offset by increasing temperature variation. Lastly, we infer that range shifts over the last ~20,000 years are likely to reflect periods of both sympatry and allopatry, and that future climate conditions will favor increased range overlap among the two species in coastal regions and a decreased probability of *R. ovata* occurrence in Arizona.

4.1 | Morphology

There is a clear difference among *R. integrifolia* and *R. ovata* based on leaf morphology, and localities containing both parental species display intermediate features (Figure 2). This intermediacy is likely to indicate the degree to which the genome of each individual is introgressed; that is, how much of the genome is represented by each parental species. Based on our sampling, introgressant populations occur at mid-elevation localities, approximately 300–400 m above sea level (Figure S1). The observed patterns of morphological intermediacy reflect those in other systems, including introgression in California (e.g., Albert, D'Antonio, & Schierenbeck, 1997; Dodd & Afzal-Rafii, 2004; Dorado, Rieseberg, & Arias, 1992).

It is unclear what positive or negative fitness consequences there may be for introgressive hybridization in this species complex. It remains to be tested whether selection against alleles from the other species may limit the spread of these alleles between parental species in the allopatric portion of their ranges, or if intermediate hybrid populations serve as a bridge for the exchange of adaptive alleles (Barton & Hewitt, 1985; Rieseberg & Burke, 2001). Although we found morphological differentiation (P_{ST}) to outrank neutral genetic differentiation (Φ_{ST}) above a certain heritability threshold (i.e., $c/h^2 =$

0.2 and 0.4 for ITS and plastid DNA, respectively; Figure 6), it remains unclear whether this is caused by extensive phenotypic plasticity or adaptive genetic variation.

4.2 | Leaf area and environmental variation

Leaf area has long been recognized as an important functional trait at the inter- and intraspecific levels (e.g., Osnas et al., 2018; Osnas, Lichstein, Reich, & Pacala, 2013). Young (1974) noted a possible relationship between latitude and leaf size in *R. ovata*, based on limited sampling of three localities. We have explicitly tested this pattern in the context of abiotic environmental variation, which represents a more accurate approach than using latitude, longitude and elevation as proxies for environmental variation. Our analysis of 19 sampling localities highlights differences among groupings (e.g., *R. ovata*, *R. integrifolia* and introgressant populations) as the primary determinants of leaf area (as corroborated by Figure 2), but also suggests an association between overall precipitation ($PC1_{precip}$) and leaf area (Table 3). Although weak, this association is negative, with smaller leaves at localities with higher overall precipitation. However, there is significant interaction between overall temperature and overall precipitation, suggesting these two factors may jointly influence leaf area. The overall precipitation-leaf area association is offset by temperature variation; that is, warmer, wetter areas tend to harbor populations with smaller leaves, but local climates with more drastic temperature swings show an opposite trend (Table3).

In general across land plants, species in xeric regions tend to have leaves that are small (e.g., Givnish, 1979), succulent, dissected or even absent (e.g., cacti and euphorbias), and it seems counterintuitive that leaf area would decrease with increasing precipitation in this species complex. In fact, we found the opposite of what has been observed across many other species, as larger leaves are thought to shed heat more slowly due to a larger boundary layer in hot, arid environments, thus posing a risk for overheating and extensive evaporative water loss (Schuepp, 1993). *Rhus ovata* has thick, waxy leaves that fold adaxially along the midrib during the hottest, driest months, which is likely to represent an adaptation to seasonally extreme heat and aridity in chaparral habitats (e.g., Herbert & Larsen, 1985). However, *R. ovata* experiences temperatures below freezing, especially at high-elevation inland localities (Boorse, Ewers, & Davis, 1998; Montalvo et al., 2017), and thus the relationship observed between leaf area, precipitation and temperature may reflect a complex tradeoff between climatic extremes. Other factors not included in our analysis, such as soil fertility, grazing pressure and density dependence, may interact with abiotic climatic factors and provide a clearer picture of the determinants of leaf area in *Rhus*. There are some localities at which *R. integrifolia*, *R. ovata* and their hybrids occur within close proximity, with steep elevational gradients (e.g., in the Santa Monica Mountains of California). These areas provide the ideal grounds for "natural experiments" to study the dynamics of leaf area as it relates to putative adaptations to temperature, precipitation and the maintenance of hybrid zones.

4.3 | Population genetics

Nuclear ITS and two plastid markers display clear patterns of allele sharing at localities with hypothesized introgression, reflecting a congruent pattern to that of morphological intermediacy (Figures 2–4). However, these shared haplotypes are not restricted to localities in which plants display intermediate morphologies; indeed, the two most common ITS and plastid haplotypes are widespread, being shared at localities corresponding to either morphologically distinct *R. integrifolia* or Californian *R. ovata*. Widespread ITS allele sharing across the network differs somewhat from the pattern based on plastid DNA. For example, the most common ITS haplotype among *R. integrifolia* localities is also found in CA and AZ localities of *R. ovata*. Likewise, the most common ITS haplotype in AZ localities is also found in Californian *R. ovata* localities, and even in *R. integrifolia*. Within *R. ovata*, which is disjunct from California to Arizona, four of six Californian localities contain multiple plastid haplotypes, whereas all Arizonan populations contain a single, identical haplotype. Three of five Arizonan localities contain a single, common ITS haplotype. This finding suggests a potential bottleneck, or that smaller effective population sizes in Arizona may be prone to the effects of genetic drift, resulting in overall lower genetic diversity there.

Overall, a weaker population structure for ITS than for plastid DNA could be driven by two factors: larger effective population sizes and unsorted ancestral polymorphism for nuclear DNA than for organellar DNA (Avise, 2000; Hare, 2001; McCauley, 1995; Palumbi & Baker, 1994; Palumbi, Cipriano, & Hare, 2001), or a greater interpopulation dispersal range for pollen versus seeds (e.g., Ennos, 1994; Hamilton, 1999; Kartzinel, Shefferson, & Trapnell, 2013). Both *Rhus* species are predominantly pollinated by bees (Moldenke & Neff, 1974; Young, 1972), whereas seeds are dispersed by mammals and birds (Lloret & Zedler, 1991; Rowe & Blazich, 2008). Our findings are congruent with a hypothesis in which barriers to pollen dispersal are low among populations of

both species and between them, albeit with decreased fecundity for "hybrid" individuals, as observed in previous experimental crosses (Young, 1972). Negative fecundity barriers may be overcome if pollen flow occurs frequently enough over long enough distances. Seed dispersal, on the other hand, may be limited by successful recruitment (e.g., Arrieta & Suárez, 2006; Dunne & Parker, 1999), which may be amplified if avian or mammalian vectors travel long distances, dispersing seeds at unfavorable localities with different local environmental conditions. This is especially pertinent if local conditions (soil, temperature, moisture, fire regime and frost formation) vary enough across sites such that environmental differences between source and sink sites suppress successful colonization by immigrant propagules, which may not be able to compete in new localities. Boorse et al. (1998) conducted the only study documenting putative evidence for local adaptation in *R. ovata*: plants from a site with lower minimum winter temperatures were significantly less susceptible to freezing damage than plants from a warmer site in the same region of coastal California. Furthermore, leaves of seedlings were much more susceptible to freezing than those from adult plants, possibly representing a barrier to successful establishment by propagules from nearby warmer habitats. Reciprocal transplants using seeds of *R. integrifolia*, *R. ovata* and their hybrids could yield useful data on whether recruitment is limited by local adaptation, and whether this has implications for population structure as it relates to seed dispersal and successful establishment.

Unsorted ancestral polymorphism would seem unlikely in this case to be the sole explanation for widely shared ITS haplotypes, given the previously estimated divergence time of ~3.1 mya between *R. integrifolia* and *R. ovata* (Yi et al., 2004). Widespread pollen flow (both historical and contemporary), potential environmental barriers to external propagule recruitment in established populations, and differences in plastid versus nuclear DNA effective population sizes may all contribute to the discrepancy in population structure among localities. Genome-scale data would allow several hypotheses to be tested regarding demographic history, patterns of gene flow between the two species and their introgressants, the adaptive value (if any) of introgression, and detailed analysis of maintenance of hybrid zones between the two species in California (e.g., Wong et al., 2020). For example, a comparison of which regions of the genome have experienced higher or lower rates of introgression would be particularly insightful, especially in the context of putatively adaptive or maladaptive introgression (e.g., Grant & Grant, 1998; Rieseberg & Burke, 2001). Furthermore, these data would provide the level of resolution needed for the construction of historical demographic models under ancestral and contemporary gene flow versus retained ancestral polymorphism.

4.4 | Species distribution modeling

Our species distribution models accurately capture the ranges of both species despite the lack of significant niche differentiation between them. The lack of niche differences between our MAXENT distribution models based on the RTR-MO test is likely to reflect the existence of hybrid/introgressed populations of *R. integrifolia* and *R. ovata* and their high degree of niche similarity in coastal regions (Figure 7). Hybrid populations present a problem for species distribution models; specimens from GBIF are identified either as *R. integrifolia* or *R. ovata* but do not include information on hybrid status. A meticulous analysis of morphology, and perhaps even genetic variation, from herbarium specimens might improve resolution of future species distribution models in the *R. integrifolia-ovata* complex, by allowing populations with evidence of hybrid introgressants to be treated as a separate category. However, even this approach may be an oversimplification, because the degree to which each population is introgressed is likely to vary across regions of overlap among the parental species (Arnold, 1997), and thus the application of a hybrid index on a continuous scale may be more appropriate (e.g., Cullingham, James, Cooke, & Coltman, 2012).

Based on our models, we infer a northward shift in the distribution of *R. integrifolia*, as well as a higher concentration of occurrence immediately along the Californian coast forecasted for 2070, for both the best- and worst-case projections of future atmospheric CO_2 levels (Figure 7). Thus, the distribution of *R. integrifolia* is likely to be forced by climate change to shift into one of the most densely populated regions in North America, where human development continues to compromise coastal habitats. For *R. ovata* we infer a similar northward shift for interior populations in Arizona, and a gradually decreasing occurrence probability in that region. Our models also infer an increased occurrence probability along the Californian coast and in northern Baja California for *R. ovata*. Riordan, Montalvo, and Beyers (2018) used species distribution modeling in several southern Californian chaparral plant species and predicted that suitable habitat would generally remain stable in the future for *R. ovata*. However, they also predicted that habitat gains in low-elevation areas for *R. ovata* are likely to coincide with future human development and that population fragmentation is predicted to increase, with implications for gene flow and local adaptation.

Taken as a whole, our 2070 forecast indicates that both species will be forced into a higher degree of sympatry, possibly increasing the occurrence of introgression. A worst-case scenario would include decreasing occurrence probability in the allopatric part of the range for *R. ovata* (i.e., Arizona), coupled with the prediction that *R. integrifolia* and *R. ovata* will be pushed into coastal regions. Although it is impossible to predict exactly what will happen in the future, global climate change may contribute to the erosion of locally adapted variants and possibly species boundaries by increasing the frequency of hybridization among these two species. This finding highlights the need for investigation of the importance of local adaptation within each species, and the adaptive consequences of potentially increased levels of hybridization among them, for example via common garden experiments, reciprocal transplants with experimental crosses and genomic analysis.

4.5 | Taxonomic implications

Hybridization has long presented challenges for species delimitation, especially concerning the Biological Species Concept (e.g., Mallet, 2005). Although *R. ovata* and *R. integrifolia* are clearly distinct in regions of allopatry, the same cannot be said within regions of sympatry. The two species become nearly indistinguishable in the latter, forming a continuous gradation in morphology, genetic variation and niche overlap. The evidence presented here does not warrant specific taxonomic changes, but it does suggest that hybrid status should be considered when depositing new collections in specimen databases. Popular instruments for "crowdsourcing" of species occurrence data could be used to distinguish between more "pure" forms of each species and hybrid introgressants. For example, using the application iNaturalist (https://www.inaturalist.org/), there are 170 records of *R. integrifolia* × *ovata* (likely to be an underestimate of actual abundance), 5715 of *R. integrifolia* and 3591 of *R. ovata* (last accessed April 14, 2020). Although these types of observations have obvious biases (e.g., clustered near population centers or public lands; for example Dickinson et al., 2012), if properly verified by an expert or via machine learning (e.g., Kaur & Tulsi, 2019; Priya, Balasaravanan, & Thanamani, 2012; Wilf et al., 2016) they may ultimately improve distribution models for hybridizing species, including *R. integrifolia* and *R. ovata*.

The acquisition of genome-scale variation and implementation of hybrid zone analyses (sensu Abbott, 2017; Ma et al., 2019; Wong et al., 2020) should be informative in determining patterns of gene flow among these two species (Taylor & Larson, 2019). Such data will allow the detection of adaptive variants, and regions of the genome that experience higher or lower levels of gene flow than regions under neutral expectations (Whitney, Ahern, Campbell, Albert, & King, 2010). Ultimately, genomic information should be used to infer the relative importance of selection in maintaining species boundaries in the face of frequent gene flow (Feder, Egan, & Nosil, 2012; Rieseberg & Burke, 2001; Suarez-Gonzalez, Lexer, & Cronk, 2018).

ACKNOWLEDGMENTS

We thank the USDA Forest Service for permission to collect samples. We also thank Ryan Percifield, Ashley Henderson and Apoorva Ravishankar (WVU Genomics Core Facility) for technical assistance, and are grateful for a CTSI Grant #U54 GM104942, which in turn provides financial support to the Genomics Core Facility. Funding was provided by the West Virginia University Department of Biology, the WVU Eberly College of Arts and Sciences, a WVU Program to Stimulate Competitive Research (PSCoR) award, and NSF EPSCoR Award # 1920858 to CB.

CONFLICT OF INTERESTS

The authors declare no conflicts of interest.

ORCID

Craig F. Barrett https://orcid.org/0000-0001-8870-3672
Heather M. Stephens https://orcid.org/0000-0003-3472-216X

REFERENCES

Abbott, R., Albach, D., Ansell, S., Arntzen, J. W., Baird, S. J. E., Bierne, N., ... Zinner, D. (2013). Hybridization and speciation. *Journal of Evolutionary Biology*, *26*, 229–246. https://doi.org/10.1111/j.1420-9101.2012.02599.x

Abbott, R. J. (2017). Plant speciation across environmental gradients and the occurrence and nature of hybrid zones. *Journal of Systematics & Evolution*, *55*, 238–258.

Adobe Inc. (2019). *Adobe illustrator*, San Jose, California, CA: Retrieved from https://adobe.com/products/illustrator

Aizawa, M., & Iwaizumi, M. G. (2020). Natural hybridization and introgression of *Abies firma* and *Abies homolepis* along the altitudinal gradient and genetic insights into the origin of *Abies umbellata*. *Plant Species Biology*, *35*, 147–157. https://doi.org/10.1111/1442-1984.12269

Albert, M. E., D'Antonio, C. M., & Schierenbeck, K. A. (1997). Hybridization and introgression in *Carpobrotus* spp. (Aizoaceae) in California. I. Morphological evidence. *American Journal of Botany*, *84*, 896–904. https://doi.org/10.2307/2446279

Arnold, M. L. (1997). *Natural hybridization and evolution*. New York, NY: Oxford University Press Inc.

Arnold, M. L. (2004). Transfer and origin of adaptations through natural hybridization: Were Anderson and Stebbins right? *The Plant Cell*, *16*, 562–570. https://doi.org/10.1105/tpc.160370

Arrieta, S., & Suárez, F. (2006). Marginal holly (*Ilex aquifolium* L.) populations in Mediterranean Central Spain are constrained by a low-seedling recruitment. *Flora - Morphology, Distribution, Functional Ecology of Plants*, *201*, 152–160. https://doi.org/10.1016/j.flora.2005.05.002

Avise, J. (2000). *Phylogeography: The history and formation of species*. Cambridge, MA: Harvard University Press.

Barkley, F. A. (1937). A monographic study of *Rhus* and its immediate allies in north and Central America, including the West Indies. *Annals of the Missouri Botanical Garden*, *24*, 265–498. https://doi.org/10.2307/2394183

Barrett, S. C. H. (2002). The evolution of plant sexual diversity. *Nature Reviews Genetics*, *3*, 274–284. https://doi.org/10.1038/nrg776

Barrett, C. F., Sinn, B. T., King, L. T., Medina, J. C., Bacon, C. D., Lahmeyer, S. C., & Hodel, D. R. (2019). Phylogenomics, biogeography and evolution in the American genus *Brahea* (Arecaceae). *Botanical Journal of the Linnean Society*, *190*, 242–259. https://doi.org/10.1093/botlinnean/boz015

Barton, N. H., & Hewitt, G. M. (1985). Analysis of hybrid zones. *Annual Review of Ecology and Systematics*, *16*, 113–148. https://doi.org/10.1146/annurev.es.16.110185.000553

da Silva, B. S., & da Silva, A. (2018). Pstat: An R package to assess population differentiation in phenotypic traits. *The R Journal*, *10*, 447–454. https://doi.org/10.32614/RJ-2018-010

Boorse, G. C., Ewers, F. W., & Davis, S. D. (1998). Response of chaparral shrubs to below-freezing temperatures: Acclimation, ecotypes, seedlings vs. adults. *American Journal of Botany*, *85*, 1224–1230. https://doi.org/10.2307/2446631

Brommer, J. E. (2011). Whither P_{ST}? The approximation of Q_{ST} by P_{ST} in evolutionary and conservation biology. *Journal of Evolutionary Biology*, *24*, 1160–1168. https://doi.org/10.1111/j.1420-9101.2011.02268.x

Burke, J. M., Voss, T. J., & Arnold, M. L. (1998). Genetic interactions and natural selection in Louisiana iris hybrids. *Evolution*, *52*, 1304–1310. https://doi.org/10.1111/j.1558-5646.1998.tb02012.x

Clement, M., Posada, D., & Crandall, K. A. (2000). TCS: a computer program to estimate gene genealogies. *Molecular Ecology*, *9*, 1657–1659. https://doi.org/10.1046/j.1365-294x.2000.01020.x

Cullingham, C. I., James, P. M. A., Cooke, J. E. K., & Coltman, D. W. (2012). Characterizing the physical and genetic structure of the lodgepole pine × jack pine hybrid zone: Mosaic structure and differential introgression. *Evolutionary Applications*, *5*, 879–891. https://doi.org/10.1111/j.1752-4571.2012.00266.x

Dellicour, S., & Mardulyn, P. (2014). Spads 1.0: A toolbox to perform spatial analyses on DNA sequence data sets. *Molecular Ecology Resources*, *14*, 647–651. https://doi.org/10.1111/1755-0998.12200

Dickinson, J. L., Shirk, J., Bonter, D., Bonney, R., Crain, R. L., Martin, J., … Purcell, K. (2012). The current state of citizen science as a tool for ecological research and public engagement. *Frontiers in Ecology and the Environment*, *10*, 291–297. https://doi.org/10.1890/110236

Dodd, R. S., & Afzal-Rafii, Z. (2004). Selection and dispersal in a multispecies oak hybrid zone. *Evolution*, *58*, 261–269. https://doi.org/10.1111/j.0014-3820.2004.tb01643.x

Dorado, O., Rieseberg, L. H., & Arias, D. M. (1992). Chloroplast DNA introgression in southern California sunflowers. *Evolution*, *46*, 566–572. https://doi.org/10.1111/j.1558-5646.1992.tb02061.x

Doyle, J. J., & Doyle, J. L. (1987). A rapid DNA isolation procedure for small quantities of fresh leaf tissue. *Phytochemical Bulletin*, *19*, 11–15.

Dunne, J. A., & Parker, V. T. (1999). Species-mediated soil moisture availability and patchy establishment of *Pseudotsuga menziesii* in chaparral. *Oecologia*, *119*, 36–45. https://doi.org/10.1007/s004420050758

Ellstrand, N. C. (2003). Current knowledge of gene flow in plants: Implications for transgene flow. *Philosophical Transactions of the Royal Society B: Biological Sciences*, *358*, 1163–1170. https://doi.org/10.1098/rstb.2003.1299

Ellstrand, N. C., & Schierenbeck, K. A. (2000). Hybridization as a stimulus for the evolution of invasiveness in plants? *Proceedings of the National Academy of Sciences*, *97*, 7043–7050. https://doi.org/10.1073/pnas.97.13.7043

Ennos, R. A. (1994). Estimating the relative rates of pollen and seed migration among plant populations. *Heredity*, *72*, 250–259. https://doi.org/10.1038/hdy.1994.35

Excoffier, L., Smouse, P. E., & Quattro, J. M. (1992). Analysis of molecular variance inferred from metric distances among DNA haplotypes: Application to human mitochondrial DNA restriction data. *Genetics*, *131*, 479–491.

Excoffier, L., & Lischer, H. E. L. (2010). Arlequin suite ver. 3.5: A new series of programs to perform population genetics analyses under Linux and windows. *Molecular Ecology Resources*, *10*, 564–567. https://doi.org/10.1111/j.1755-0998.2010.02847.x

Feder, J. L., Egan, S. P., & Nosil, P. (2012). The genomics of speciation-with-gene-flow. *Trends in Genetics*, *28*, 342–350. https://doi.org/10.1016/j.tig.2012.03.009

Fick, S. E., & Hijmans, R. J. (2017). WorldClim 2: New 1-km spatial resolution climate surfaces for global land areas. *International Journal of Climatology*, *37*, 4302–4315. https://doi.org/10.1002/joc.5086

Flot, J.-F. (2010). SeqPhase: A web tool for interconverting phase input/output files and fasta sequence alignments. *Molecular Ecology Resources*, *10*, 162–166. https://doi.org/10.1111/j.1755-0998.2009.02732.x

Freeman, D. C., Doust, J. L., El-Keblawy, A., Miglia, K. J., & McArthur, E. D. (1997). Sexual specialization and inbreeding avoidance in the evolution of dioecy. *Botanical Review*, *63*, 65–92.

Gavrilets, S., & Cruzan, M. B. (1998). Neutral gene flow across single locus clines. *Evolution*, *52*, 1277–1284. https://doi.org/10.1111/j.1558-5646.1998.tb02009.x

Gent, P. R., Danabasoglu, G., Donner, L. J., Holland, M. M., Hunke, E. C., Jayne, S. R., … Zhang, M. (2011). The community climate system model version 4. *Journal of Climate*, *24*, 4973–4991. https://doi.org/10.1175/2011JCLI4083.1

Givnish, T. (1979). On the adaptive significance of leaf form. In O. T. Solbrig, S. Jain, G. B. Johnson, & P. H. Raven (Eds.), *Topics in plant population biology* (pp. 375–407). London, England: Palgrave. https://doi.org/10.1007/978-1-349-04627-0_17

Grant, B. R., & Grant, P. R. (1998). In D. J. Howard & S. H. Berlocher (Eds.), *Endless forms: Species and speciation Hybridization and speciation in Darwin's finches: The role of sexual imprinting on a culturally transmitted trait* (pp. 404–422). New York, NY: Oxford University Press.

Gower, J. C. (1971). A general coefficient of similarity and some of its properties. *Biometrics*, *27*, 857–871.

Hijmans, R. J. (2019). Raster: Geographic data analysis and modeling. R Package Version 3.0-12. Retrieved from https://CRAN.R-project.org/package=raster

Hamilton, M. B. (1999). Tropical tree gene flow and seed dispersal. *Nature*, *401*, 129–130. https://doi.org/10.1038/43597

Hammer, Ø., Harper, D. A. T., & Ryan, P. D. (2001). PAST: Paleontological Statistics Software Package for education and data analysis. *Palaeontologia Electronica*, *4*. Retieved from http://palaeo-electronica.org/2001_1/past/issue1_01.htm

Hare, M. P. (2001). Prospects for nuclear gene phylogeography. *Trends in Ecology & Evolution*, *16*, 700–706. https://doi.org/10.1016/S0169-5347(01)02326-6

Hegarty, M. J., & Hiscock, S. J. (2005). Hybrid speciation in plants: New insights from molecular studies. *New Phytologist*, *165*, 411–423. https://doi.org/10.1111/j.1469-8137.2004.01253.x

Herbert, T. J., & Larsen, P. B. (1985). Leaf movement in *Calathea lutea* (Marantaceae). *Oecologia*, *67*, 238–243. https://doi.org/10.1007/BF00384292

Hoskin, C. J., Higgie, M., McDonald, K. R., & Moritz, C. (2005). Reinforcement drives rapid allopatric speciation. *Nature*, *437*, 1353–1356. https://doi.org/10.1038/nature04004

Hugh-Jones, D. (2020). HuxTable: Easily create and style tables for LaTeX, HTML and other formats. R Package Version 4.7.1. Retrieved from https://CRAN.R-project.org/package=huxtable

Kartzinel, T. R., Shefferson, R. P., & Trapnell, D. W. (2013). Relative importance of pollen and seed dispersal across a Neotropical mountain landscape for an epiphytic orchid. *Molecular Ecology*, *22*, 6048–6059. https://doi.org/10.1111/mec.12551

Kaur, S., & Tulsi, P. K. (2019). Plant species identification based on plant leaf using computer vision and machine learning techniques. *Journal of Multimedia Information System*, *6*, 49–60. https://doi.org/10.33851/JMIS.2019.6.2.49

Katoh, K., & Standley, D. M. (2013). MAFFT Multiple Sequence Alignment Software Version 7: Improvements in Performance and Usability. *Molecular Biology and Evolution*, *30*, 772–780. https://doi.org/10.1093/molbev/mst010.

Leigh, J. W., & Bryant, D. (2015). PopArt: Full-feature software for haplotype network construction. *Methods in Ecology and Evolution*, *6*, 1110–1116. https://doi.org/10.1111/2041-210X.12410

Lloret, F., & Zedler, P. H. (1991). Recruitment pattern of *Rhus integrifolia* populations in periods between fire in chaparral. *Journal of Vegetation Science*, *2*, 217–230. https://doi.org/10.2307/3235954

Long J. A. (2019). Jtools: Analysis and presentation of social scientific data. R Package Version 2.0.1. Retrieved from https://cran.r-project.org/package=jtools

Ma, Y., Wang, J., Hu, Q., Li, J., Sun, Y., Zhang, L., … Mao, K. (2019). Ancient introgression drives adaptation to cooler and drier mountain habitats in a cypress species complex. *Communications Biology*, *2*, 213.

Mallet, J. (2005). Hybridization as an invasion of the genome. *Trends in Ecology & Evolution*, *20*, 229–237. https://doi.org/10.1016/j.tree.2005.02.010

Mavárez, J., Salazar, C. A., Bermingham, E., Salcedo, C., Jiggins, C. D., & Linares, M. (2006). Speciation by hybridization in *Heliconius* butterflies. *Nature*, *441*, 868–871. https://doi.org/10.1038/nature04738

McCauley, D. E. (1995). The use of chloroplast DNA polymorphism in studies of gene flow in plants. *Trends in Ecology & Evolution*, *10*, 198–202. https://doi.org/10.1016/s0169-5347(00)89052-7

Miller, A. J., Young, D. A., & Wen, J. (2001). Phylogeny and biogeography of *Rhus* (Anacardiaceae) based on ITS sequence data. *International Journal of Plant Sciences*, *162*, 1401–1407. https://doi.org/10.1086/322948

Moldenke, A. R., and Neff, J. L. (1974). *Studies on pollination ecology and species diversity of natural California plant communities*, *III*. Technical report 74–14, International Biological Programme, Origin and Structure of Ecosystems.

Montalvo, A. M., Riordan, E. C., & Beyers, J. L. (2017). *Plant profile for Rhus ovata. Native Plant Recommendations for Southern California Ecoregions*. Riverside, CA: *Riverside-Corona Resource Conservation District and U.S. Department of Agriculture*, Forest Service, Pacific Southwest Research Station. Retrieved from https://www.rcrcd.org/plant-profiles

Munz, P. A., & Keck, D. D. (1959). *A California Flora*. Berkeley, CA: University of California Press.

Osnas, J. L. D., Katabuchi, M., Kitajima, K., Wright, S. J., Reich, P. B., Van Bael, S. A., … Lichstein, J. W. (2018). Divergent drivers of leaf trait variation within species, among species, and among functional groups. *Proceedings of the National Academy of Sciences*, *115*, 5480–5485. https://doi.org/10.1073/pnas.1803989115

Osnas, J. L. D., Lichstein, J. W., Reich, P. B., & Pacala, S. W. (2013). Global leaf trait relationships: Mass, area, and the leaf economics spectrum. *Science*, *340*, 741–744. https://doi.org/10.1126/science.1231574

Palumbi, S. R., & Baker, C. S. (1994). Contrasting population structure from nuclear intron sequences and mtDNA of humpback whales. *Molecular Biology and Evolution*, *11*, 426–435. https://doi.org/10.1093/oxfordjournals.molbev.a040115

Palumbi, S. R., Cipriano, F., & Hare, M. P. (2001). Predicting nuclear gene coalescence from mitochondrial data: The three-times rule. *Evolution*, *55*, 859–868. https://doi.org/10.1111/j.0014-3820.2001.tb00603.x

Petit, R. J., & Excoffier, L. (2009). Gene flow and species delimitation. *Trends in Ecology & Evolution*, *24*, 386–393. https://doi.org/10.1016/j.tree.2009.02.011

Pebesma, E.J., and R.S. Bivand, 2005. Classes and methods for spatial data in R. *R News 5*. Retrieved from https://cran.r-project.org/doc/Rnews/

Phillips, S. J., Anderson, R. P., & Schapire, R. E. (2006). Maximum entropy modeling of species geographic distributions. *Ecological Modelling*, *190*, 231–259. https://doi.org/10.1016/j.ecolmodel.2005.03.026

Phillips, S. J., Anderson, R. P., Dudík, M., Schapire, R. E., & Blair, M. E. (2017). Opening the black box: An open-source release of Maxent. *Ecography*, *40*, 887–893. https://doi.org/10.1111/ecog.03049

Priya, C. A., Balasaravanan, T., & Thanamani, A. S. (2012). An efficient leaf recognition algorithm for plant classification using support vector machine. International conference on pattern recognition, informatics and medical engineering (PRIME-2012) (pp. 428–432). https://doi.org/10.1109/ICPRIME.2012.6208384

Reist, J. (2011). An empirical evaluation of several univariate methods that adjust for size variation in morphometric data.

Canadian Journal of Zoology, *63*, 1429–1439. https://doi.org/10.1139/z85-213

Rieseberg, L. H., & Soltis, D. E. (1991). Phylogenetic consequences of cytoplasmic gene flow in plants. *Evolutionary Trends in Plant*, *5*, 65–84.

Rieseberg, L., Van Fossen, C., & Desrochers, A. (1995). Hybrid speciation accompanied by genomic reorganization in wild sunflowers. *Nature*, *375*, 313–316. https://doi.org/10.1038/375313a0

Rieseberg, L. H., Whitton, J., & Gardner, K. (1999). Hybrid zones and the genetic architecture of a barrier to gene flow between two sunflower species. *Genetics*, *152*, 713.

Rieseberg, L. H., & Burke, J. M. (2001). The biological reality of species: Gene flow, selection, and collective evolution. *Taxon*, *50*, 47–67. https://doi.org/10.2307/1224511

Riordan E. C., Montalvo A. M., & Beyers J. L. (2018). Using species distribution models with climate change scenarios to aid ecological restoration decision making for southern California shrublands. *Res. Pap. PSW-RP-270*. Albany, CA: U.S. Department of Agriculture, Forest Service, Pacific Southwest Research Station. Retrieved from https://www.fs.fed.us/psw/publications/documents/psw_rp270/psw_rp270.pdf.

Rowe, D. B., & Blazich, F. A. (2008). *Rhus* L., Sumac. In F. T. Bonner & R. P. Karrfalt (Eds.), *The woody plant seed manual. Agr. Hdbk 727* (pp. 954–960). Washington, DC: US Department of Agriculture - Foreign Agriculture Service.

Rueden, C. T., Schindelin, J., Hiner, M. C., DeZonia, B. E., Walter, A. E., Arena, E. T., & Eliceiri, K. W. (2017). ImageJ2: ImageJ for the next generation of scientific image data. *BMC Bioinformatics*, *18*, 529. https://doi.org/10.1186/s12859-017-1934-z

Saccheri, I., & Hanski, I. (2006). Natural selection and population dynamics. *Trends in Ecology & Evolution*, *21*, 341–347. https://doi.org/10.1016/j.tree.2006.03.018

Schuepp, P. H. (1993). Tansley review no. 59, leaf boundary layers. *New Phytologist*, *125*, 477–507. https://doi.org/10.1111/j.1469-8137.1993.tb03898.x

Slatkin, M. (1987). Gene flow and the geographic structure of natural populations. *Science*, *236*, 787–792. https://doi.org/10.1126/science.3576198

Soltis, P. S., & Soltis, D. E. (2009). The role of hybridization in plant speciation. *Annual Review of Plant Biology*, *60*, 561–588. https://doi.org/10.1146/annurev.arplant.043008.092039

Sork, V. L. (2016). Gene flow and natural selection shape spatial patterns of genes in tree populations: Implications for evolutionary processes and applications. *Evolutionary Applications*, *9*, 291–310. https://doi.org/10.1111/eva.12316

Stebbins, G. L. (1969). The significance of hybridization for plant taxonomy and evolution. *Taxon*, *18*, 26–35. https://doi.org/10.2307/1218589

Stephens, M., Smith, N. J., & Donnelly, P. (2001). A new statistical method for haplotype reconstruction from population data. *The American Journal of Human Genetics*, *68*(4), 978–989. https://doi.org/10.1086/319501

Suarez-Gonzalez, A., Lexer, C., & Cronk, Q. C. B. (2018). Adaptive introgression: A plant perspective. *Biology Letters*, *14*, 20170688. https://doi.org/10.1098/rsbl.2017.0688

Taylor, S. A., & Larson, E. L. (2019). Insights from genomes into the evolutionary importance and prevalence of hybridization in nature. *Nature Ecology & Evolution*, *3*, 170–177. https://doi.org/10.1038/s41559-018-0777-y

White, B. T., Lee, S., & Taylor, J. (1990). Amplification and direct sequencing of fungal ribosomal RNA genes for phylogenetics. In M. A. Innis, D. H. Gelfand, J. J. Sninsky, & T. J. White (Eds.), *PCR protocols: A guide to methods and applications* (pp. 315–322). New York, NY: Academic Press Inc.

Whitney, K. D., Ahern, J. R., Campbell, L. G., Albert, L. P., & King, M. S. (2010). Patterns of hybridization in plants. *Perspectives in Plant Ecology, Evolution and Systematics*, *12*, 175–182. https://doi.org/10.1016/j.ppees.2010.02.002

Wickham, H. (2016). *ggplot2: Elegant graphics for data analysis*. New York, NY: Springer-Verlag. https://doi.org/10.1007/978-3-319-24277-4

Wilf, P., Zhang, S., Chikkerur, S., Little, S. A., Wing, S. L., & Serre, T. (2016). Computer vision cracks the leaf code. *Proceedings of the National Academy of Sciences of the United States of America*, *113*, 3305–3310. https://doi.org/10.1073/pnas.1524473113

Wong, E. L. Y., Nevado, B., Osborne, O. G., Papadopulos, A. S. T., Bridle, J. R., Hiscock, S. J., & Filatov, D. A. (2020). Strong divergent selection at multiple loci in two closely related species of ragworts adapted to high and low elevations on Mount Etna. *Molecular Ecology*, *29*, 394–412.

Yi, T., Miller, A. J., & Wen, J. (2004). Phylogenetic and biogeographic diversification of *Rhus* (Anacardiaceae) in the northern hemisphere. *Molecular Phylogenetics and Evolution*, *33*, 861–879. https://doi.org/10.1016/j.ympev.2004.07.006

Young, D. A. (1972). The reproductive biology of *Rhus integrifolia* and *Rhus ovata* (Anacardiaceae). *Evolution*, *26*, 406–414. https://doi.org/10.1111/j.1558-5646.1972.tb01945.x

Young, D. A. (1974). Introgressive hybridization in two southern California species of *Rhus* (Anacardiaceae). *Brittonia*, *26*, 241. https://doi.org/10.2307/2805727

Zizka, A., Silvestro, D., Andermann, T., Azevedo, J., Ritter, C. D., Edler, D., ... Antonelli, A. (2019). CoordinateCleaner: Standardized cleaning of occurrence records from biological collection databases. *Methods in Ecology and Evolution*, *10*, 744–751. https://doi.org/10.1111/2041-210X.13152

SUPPORTING INFORMATION

Additional supporting information may be found online in the Supporting Information section at the end of this article.

How to cite this article: Barrett CF, Lambert J, Santee MV, et al. Genetic, morphological, and niche variation in the widely hybridizing *Rhus integrifolia-Rhus ovata* species complex. *Plant Species Biol*. 2020;1–19. https://doi.org/10.1111/1442-1984.12293